# NAD-malic enzymes of *Arabidopsis thaliana* display distinct kinetic mechanisms that support differences in physiological control

Q1

Marcos A. TRONCONI*, Mariel C. GERRARD WHEELER*, Verónica G. MAURINO†, María F. DRINCOVICH* and Carlos S. ANDREO*[1]

*Centro de Estudios Fotosintéticos y Bioquímicos (CEFOBI), Universidad Nacional de Rosario, Suipacha 531, Rosario, Argentina, and †Botanisches Institut, Universität zu Köln, Zülpicher Str. 47b, 50674, Cologne, Germany.

The *Arabidopsis thaliana* genome contains two genes encoding NAD-MEs [NAD-dependent malic enzymes; *NAD-ME1* (TAIR accession number At4G13560) and *NAD-ME2* (TAIR accession number At4G00570)]. The encoded proteins are localized to mitochondria and assemble as homo- and heterodimers *in vitro* and *in vivo*. In the present work, the kinetic mechanisms of NAD-ME1 and -ME2 homodimers and NAD-MEH (NAD-ME heterodimer) were studied as an approach to understand the contribution of these enzymes to plant physiology. Product-inhibition and substrate-analogue analyses indicated that NAD-ME2 follows a sequential ordered Bi-Ter mechanism, NAD being the leading substrate followed by L-malate. On the other hand, NAD-ME1 and NAD-MEH can bind both substrates randomly. However, NAD-ME1 shows a preferred route that involves the addition of NAD first. As a consequence of the kinetic mechanism, NAD-ME1 showed a partial inhibition by L-malate at low NAD concentrations. The analysis of a protein chimaeric for NAD-ME1 and -ME2 indicated that the first 176 amino acids are associated with the differences observed in the kinetic mechanisms of the enzymes. Furthermore, NAD-ME1, -ME2 and -MEH catalyse the reverse reaction (pyruvate reductive carboxylation) with very low catalytic activity, supporting the notion that these isoforms act only in L-malate oxidation in plant mitochondria. The different kinetic mechanism of each NAD-ME entity suggests that, for a metabolic condition in which the mitochondrial NAD level is low and the L-malate level is high, the activity of NAD-ME2 and/or -MEH would be preferred over that of NAD-ME1.

Key words: *Arabidopsis thaliana*, kinetic mechanism, malate decarboxylation, NAD-dependent malic enzyme (NAD-ME), product inhibition, pyruvate carboxylation.

## INTRODUCTION

The oxidative decarboxylation of L-malate to pyruvate and $CO_2$ is catalysed by MEs (malic enzymes) with the general requirement for a divalent cation: NADP-ME [NADP-dependent ME; EC (Enzyme Commission) number 1.1.1.40] and NAD-ME (NAD-dependent ME; EC number 1.1.1.38 or 1.1.1.39, depending on the ability, or not, to decarboxylate oxaloacetate respectively). ME is a widely distributed protein in animal and plant tissues, as well as in prokaryotic and eukaryotic microorganisms [1]. This enzyme plays a key role in the partitioning of carbon flux by regulating the levels of organic acids and reduced cofactors [2], which are involved in vital processes such as photosynthetic production of carbohydrates, respiration, biosynthesis of proteins and lipids, cellular pH regulation and defence responses [3–10]. In eukaryotic cells, NAD-MEs are found exclusively in mitochondria, whereas NADP-MEs have been found in the cytosol and plastids. The crystal structure of mitochondrial NAD-ME from humans [11] and from *Ascaris suum* [12] have been resolved and indicate that both non-plant NAD-MEs are homotetramers with a dimer-of-dimers quaternary structure. However, plant NAD-MEs differ from non-plant MEs, as they are composed of two dissimilar subunits ($\alpha$ and $\beta$) in *Solanum tuberosum* (a $C_3$ plant) [13,14], *Crassula argentea* [a CAM (crassulacean acid metabolism) plant] [14], *Urochloa panicoides* (a $C_4$ plant) [15], *Amaranthus hypochondriacus* (a $C_4$ plant) [16] and *Arabidopsis thaliana* [17,18].

Although the $\alpha$ and $\beta$ subunits contain all the motifs required for a functional NAD-ME [19], no activity was associated with the separate subunits in potato, but activity could be found in a reconstituted system [14]. Furthermore, the $\beta$ subunit was suggested to play a regulatory role [16]. More recently, the products of the two genes encoding NAD-MEs from *A. thaliana*, NAD-ME1 [TAIR (The Arabidopsis Information Resource) accession number At4G13560] and NAD-ME2 (TAIR accession number At4G00570), were characterized, showing that NAD-ME1 is more similar to the $\alpha$ subunit and NAD-ME2 is more similar to the $\beta$ subunit [17]. Individual NAD-ME1 and -ME2 proteins form active homodimers and they can associate to form an active heteromeric enzyme NAD-MEH (NAD-ME heterodimer) *in vivo* and *in vitro* [17,18]. Recombinant NAD-ME1, -ME2 and -MEH have similar optimal pH and affinities for the substrates [17,18]. However, whereas the kinetic behaviour of NAD-ME2 is hyperbolic for NAD and L-malate, NAD-ME1 and -MEH show sigmoidal kinetics, indicating cooperative binding of the substrates [17,18]. Moreover, the three enzymes are differentially regulated by key metabolites of central carbon-metabolism pathways, suggesting that each NAD-ME has a specific function in plant metabolism [18]. In this regard, although *NAD-ME1* and *ME-2* show a similar pattern of expression in

Abbreviations used: E, free enzyme; EC, Enzyme Commission; MDH, malate dehydrogenase; E-MAL, enzyme linked to L-malate; ME, malic enzyme; NAD-ME, NAD-dependent malic enzyme; NADP-ME, NADP-dependent ME; NAD-MEH, NAD-ME heterodimer; OAA, oxaloacetate; TAIR, The *Arabidopsis* Information Resource.

[1] To whom correspondence should be addressed (carlosandreo@cefobi-conicet.gov.ar)

organs of adult *A. thaliana* plants, NAD-ME1, -ME2 and -MEH proteins accumulate at different levels in separate parts of the inflorescence [17,18].

In plant mitochondria, L-malate can be metabolized by MDH (malate dehydrogenase) or by NAD-ME. Our recent work demonstrated a major participation of *Arabidopsis* NAD-MEs in nocturnal L-malate respiration [17]. However, to be able to predict L-malate fluxes through both enzymes, the knowledge of relative levels and kinetic mechanisms of both MDH and NAD-ME is required. In addition, by considering the low affinity of NAD-MEs for NAD and the levels of this compound found in plant mitochondria, it is possible that the activity of the different enzymatic entities would be regulated by changes in substrate concentrations [20,21].

In the present work, the reaction mechanisms of NAD-ME1, -ME2 and -MEH were studied by kinetic analysis. The capacity of the proteins to catalyse alternative reactions was also evaluated, as it is possible that NAD-ME can also function in the anaplerotic sense (generating L-malate from pyruvate), as was recently suggested for NADP-ME isoenzymes from *A. thaliana* [22,23]. The results presented in the present paper indicate that *A. thaliana* NAD-ME1, -ME2 and -MEH behave differently in terms of their interaction with the substrates NAD and L-malate. In addition, from the analysis of a NAD-ME1–NAD-ME-2 chimaeric protein, the N-terminal region of the primary structure was identified as being responsible for the particular kinetic behaviour of each enzyme. The possible physiological consequences of the differential properties of each NAD-ME are discussed.

## EXPERIMENTAL

### Materials

NAD(H), L-malate, oxaloacetate, fumarate, tartrate, 5′-AMP, pyruvate, Mes and reagents for SDS/PAGE were purchased from Sigma Chemical Co. (St. Louis, MO, U.S.A.). All other reagents were of analytical grade.

### Heterologous expression and purification of the recombinant enzymes

pET32 expression vectors containing the cDNA coding for the mature NAD-ME1, NAD-ME2 [17] and the chimaeric protein NAD-ME1q [18] were used to express the fusion proteins. The induction and purification of the proteins was performed as previously described [24]. For expression and purification of the NAD-MEH heterodimer, NAD-ME1 and -ME2 proteins were co-expressed as previously described [18]. The fusion proteins were digested with 0.05 to 0.075 units of enterokinase (EK-Max; Invitrogen) per miligram of protein at 16 °C for 2 h to remove the N-terminus encoded by the expression vector. The protease was eliminated using EK-Away resin (Invitrogen) according to manufacturer's instructions. The purified enzymes were concentrated using a Centricon YM-50 device (Amicon), analysed by SDS-PAGE to verify the integrity and purity, and stored at −80 °C in 50 mM Mes-NaOH pH 6.5, 5 mM $MnCl_2$, 5 mM dithiothreitol and 50 % (v/v) glycerol for further studies.

### NAD-ME oxidative decarboxylation reaction and kinetic mechanism

The oxidative decarboxylation of L-malate (forward reaction) was assayed spectrophotometrically using a standard reaction mixture containing 50 mM Mes-NaOH pH 6.5, 10 mM $MnCl_2$, 4 mM NAD and 10 mM L-malate in a final volume of 0.5 ml. The reaction was started by the addition of L-malate. One unit (U) is defined as the amount of enzyme that catalyses the formation of 1 $\mu$mol of NADH per min under the specified conditions ($\varepsilon_{340nm} = 6.22\ mM^{-1} \cdot cm^{-1}$).

Initial-velocity studies were performed by varying the concentration of one of the substrates around its $K_m$ value while keeping the other substrate concentrations at subsaturating or saturating levels. Previously reported $K_m$ (or $S_{0.5}$) values were considered (for NAD-ME1,-ME2 and -MEH: 0.5 mM and 3.0 mM for NAD and L-malate respectively; for NAD-ME1q: 0.5 mM and 0.3 mM for NAD and L-malate respectively) [8,9]. As the true substrates of malic enzymes are the free forms uncomplexed by metal ions, the data were analysed based on free concentrations of L-malate and NAD in the assay medium [25]. The following values for the dissociation constants ($K_d$) were used: $K_d$(Mn-malate) 20.0 mM and $K_d$(Mn-NAD) 12.9 mM [26].

The substrate-dependent rates were fitted to the Michaelis–Menten equation or the Hill equation by non-linear regression. Alternatively, when complex curves were obtained, initial rates were fitted to eqn (1): Q7

$$V = \frac{(a * [S]) + (b * [S]^2)}{c + (d * [S]) + (e * [S]^2)} \quad (1)$$

where [S] is the free concentration of the varying substrate and a,b,c, d and e are functions of the fixed substrate concentration and the rate constants for the reaction steps.

When both substrates were varied in a simple experiment, the data were fitted to eqns (2), (3) and (4) for a Bi-Ter ordered mechanism, a random Bi-Ter mechanism under equilibrium conditions or a steady-state random Bi-Ter kinetic mechanism Q7 respectively:

$$V = \frac{V_{max} * [A] * [B]}{([A] * [B]) + (K_m^B/[A]) + (K_s^A * K_m^B)} \quad (2)$$

$$V = \frac{V_{max} * [A] * [B]}{([A] * [B]) + (K_m^B/[A]) + (K_m^A/[B]) + (K_s^A * K_m^B)} \quad (3)$$

$$V = \frac{(a_1 * [A] * [B]) + (a_2 * [A]^2 * [B]) + (a_3 * [A] * [B]^2)}{a_4 + (a_5 * [A]) + (a_6 * [B]) + (a_7 * [A] * [B]) + (a_8 * [A]^2) + (a_9 * [B]^2) + (a_{10} * [A]^2 * [B]) + (a_{11} * [A] * [B]^2)} \quad (4)$$ Q7

where $K_s$ is the dissociation constant for the enzyme–substrate complex for substrates A and B, and $a_i$ ($i = 1$–11) involves several rate constants.

Inhibition studies were performed in a similar manner, with NADH, $CO_2$ or pyruvate as product inhibitors and tartrate or 5′-AMP as substrate analogues. Each inhibitor was held at several fixed concentrations around its inhibition constant. The inhibition constants ($K_i$) were calculated from the slope or intercept term obtained from the double-reciprocal plot of the primary graphs against the different concentrations of inhibitor used [27].

All activity assays were carried out at 30 °C in a Helios $\beta$ spectrophotometer (Unicam). Protein concentration was determined by the BioRad Protein Assay with BSA as a standard.

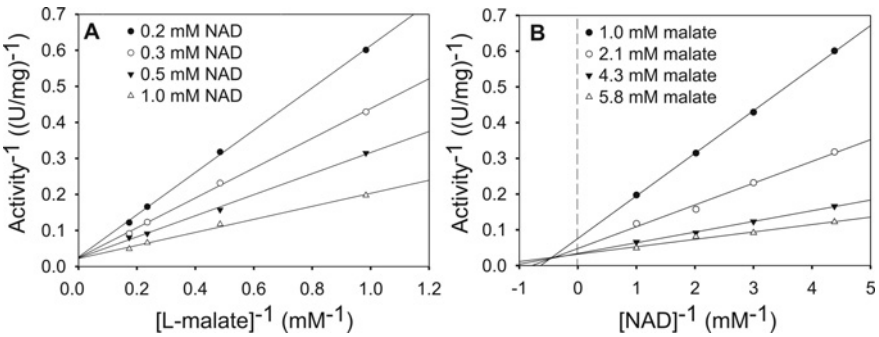


**Figure 1 Substrate-interaction kinetics of *A. thaliana* NAD-ME2**

Enzyme activity was determined at varying concentrations of L-malate (**A**) or NAD (**B**) and fixed levels of the other substrate (see insets). Double-reciprocal plots are shown, as hyperbolic kinetics were obtained in all cases. Typical results from at least three independent determinations are shown.

### Oxaloacetate decarboxylation and pyruvate reductive carboxylation

The decarboxylation of OAA (oxaloacetate) was monitored by measuring the disappearance of OAA at 260 nm ($\varepsilon_{260nm} = 850$ $M^{-1} \cdot cm^{-1}$). The assay medium contained 50 mM Mes-NaOH pH 5.5, 1 mM OAA and 10 mM $MnCl_2$ in a final volume of 0.25 ml. The reported velocities were corrected for the background rate resulting from the non-enzymatic OAA decarboxylation catalysed by the divalent metal ion.

The reductive carboxylation of pyruvate (reverse reaction) was tested in several buffer systems (50 mM Mes-NaOH, pH 6.0; 50 mM Mops-KOH pH 7.0; 50 mM Tris-HCl pH 7.5 and 50 mMTris-HCl pH 8.0) containing different concentrations of pyruvate (0.1–50 mM), NADH or NADPH (0.1–0.2 mM), $NaHCO_3$ (15–30 mM) and metal cofactor (10 mM $MnCl_2$ or $MgCl_2$) in a final volume of 0.5 ml. For each assay, the $CO_2$ concentration was calculated from the $NaHCO_3$ concentration, added using the Henderson–Hasselbach equation, at 30 °C. The linearity of the reaction was monitored in order to determine any $CO_2$ loss during the assay.

### Gel electrophoresis

SDS/PAGE was performed in 8–10 % polyacrylamide gels using the method of Laemmli [28]. Proteins were visualized with Coomassie Blue or electroblotted on to a nitrocellulose membrane for immunoblotting. Specific antibodies against *Arabidopsis* NAD-ME1 or -ME2 [17] were used for detection. Bound antibodies were visualized by linking to alkaline phosphatase-conjugated goat anti-rabbit IgG antibody according to the manufacturer's instructions (Sigma). Alkaline phosphatase activity was detected colorimetrically.

### Statistical analysis

The equation that gave the largest $F$ value and lowest standard errors was assumed to represent the model that best describes the mechanism of action of the enzyme. Initial-velocity data were fitted using the SigmaPlot 10.0 program. All determinations were performed at least in triplicate with no more than 5 % S.D. between them.

## RESULTS AND DISCUSSION

### Kinetic mechanism of NAD-ME2: ordered sequential mechanism with NAD being the leader substrate

To determine the kinetic mechanism of *A. thaliana* NAD-ME2, a series of kinetic studies were performed. When the forward enzymatic activity was measured varying NAD and L-malate concentrations, hyperbolic kinetics were obtained in all cases (results not shown). For each substrate, the representation of data according to the Lineweaver–Burk equation (1/activity versus 1/[substrate]) is shown in Figure 1. The intersecting plots suggest that the reaction course underwent a sequential mechanism as illustrated in Figure 2(A). In agreement with this, the initial-velocity data give a best fit to eqn (2) that describes a Bi-Ter ordered mechanism, as the value of statistical $F$ (2986) after fitting to this equation was higher than those obtained by fitting to eqns (3) or (4) (643 and 477 respectively). The values for the kinetic constants obtained were $k_{cat} = 46.0$ $s^{-1}$, $K_s$ NAD = 1.1 mM and $K_m$ malate = 2.6 mM.

Product-inhibition studies also indicated an ordered Bi-Ter mechanism of reaction for NAD-ME2, with NAD as the leading

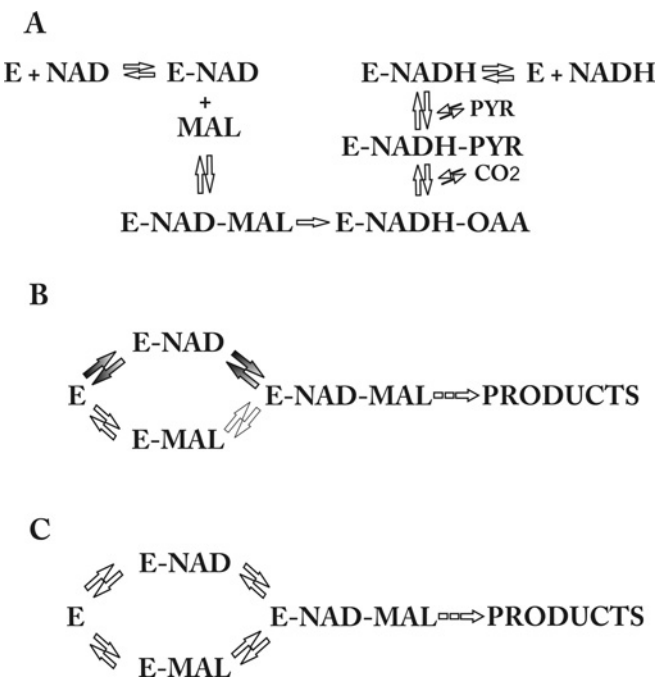


**Figure 2 Proposed kinetic mechanisms of *A. thaliana* NAD-ME1, -ME2 and -MEH** Q3

(**A**) NAD-ME2 follows a sequential ordered Bi-Ter mechanism. (**B**) NAD-ME1 can bind both substrates although the preferred route (grey arrows) involves the addition of NAD in the first place. (**C**) NAD-MEH follows a non-ordered sequential Bi-Ter mechanism. PYR, pyruvate.

**Table 1 Inhibition patterns of *A. thaliana* NAD-ME2**

The concentrations of the non-varied substrates were subsaturating and fixed at 0.6 mM NAD and 3.5 mM L-malate. $K_i$ was obtained from the gradient in the double-reciprocal plot. $K_i$' was obtained from the intercept term in the double-reciprocal plot. The full data set is shown in Supplementary Figures S1 and S2.

(a)

| | Product inhibition pattern | | |
|---|---|---|---|
| Varied substrate | NADH | Pyruvate | $CO_2$ |
| NAD | Competitive<br>$K_i = 150\ \mu M$ | Uncompetitive<br>$K_i = 11$ mM | Mixed<br>$K_i = 3$ mM, $K_i' = 11$ mM |
| L-Malate | Mixed<br>$K_i = 41\ \mu M$, $K_i' = 200\ \mu M$ | Mixed<br>$K_i = 14$ mM, $K_i' = 174$ mM | Mixed<br>$K_i = 7$ mM, $K_i' = 4$ mM |

(b)

| | Substrate-analogue inhibition pattern | |
|---|---|---|
| Varied substrate | Tartrate | 5′-AMP |
| NAD | Uncompetitive<br>$K_i = 4$ mM | Competitive<br>$K_i = 0.45$ mM |
| L-Malate | Competitive<br>$K_i = 0.8$ mM | Mixed<br>$K_i = 1.5$ mM, $K_i' = 1.4$ mM |

substrate followed by L-malate (Figure 2A). The assays were carried out by measuring the initial velocity of the reaction at varying concentrations of one substrate and a subsaturating level of the other, in the absence, or in the presence of different concentrations, of each reaction product: NADH (100 and 200 $\mu$M), pyruvate (2.5 to 50 mM) and $NaHCO_3$ (5 and 20 mM; equivalent to 2.8 mM $CO_2$ and 11.2 mM $CO_2$ respectively). Table 1 summarizes the type of inhibition displayed by the products of the reaction and shows the inhibition constants obtained.

The product-inhibition patterns showed that NADH is a competitive and mixed inhibitor with respect to NAD and L-malate respectively (Supplementary Figures S1A and S1B at http://www.BiochemJ.org/bj/430/bj430ppppadd.htm), indicating that NAD is the first binding substrate and NADH is the last product released (Figure 2A). In addition, pyruvate was an uncompetitive and mixed inhibitor with respect to NAD and L-malate respectively (Supplementary Figures S1C and S1D), indicating that it is the second product; and $CO_2$ should be the first product to leave the ternary complex (Figure 2A). Because pyruvate can only bind to the enzyme–NADH complex and not the free enzyme, an uncompetitive inhibition would be expected. However, since pyruvate is a product of the reaction, it is possible that in the presence of a high level of enzyme–NADH–pyruvate complex, some reversion of the reaction could occur, resulting in a mixed inhibition.

To provide further support for the order of addition of substrates to the active site, dead-end inhibition studies were conducted using tartrate and adenosine 5′-monophosphate (5′-AMP), compounds that structurally resemble L-malate and NAD respectively, but do not chemically react [29]. In accordance with the proposed mechanism, tartrate and 5′-AMP showed competitive inhibition patterns compared with their structural analogues (Table 1, and Supplementary Figures 2A and 2D at http://www.BiochemJ.org/bj/430/bj430ppppadd.htm). Moreover, tartrate behaved as an uncompetitive inhibitor with respect to NAD, and 5′-AMP showed mixed non-competitive inhibition with respect to L-malate (Table 1 and Supplementary Figures 2B and 2C).

The mechanism of reaction proposed for NAD-ME2 (Figure 2A) resembles those reported for NADP-MEs from $C_4$ plants such as *Pennisetum purpureum* [30] and *Zea mays* [31] and from animal sources [32–34]. However, this mechanism differs from that suggested for other NAD-MEs such as the isoforms from *C. argentea* [35] and *A. suum* [36,37], where the kinetic mechanisms were sequential with random binding of substrates and cofactors. It is worth mentioning that in the case of *C. argentea*, the enzyme used for the study was purified from leaves as a heteromer.

It is notable that NAD-ME shows the lowest affinity towards NAD when compared with other plant mitochondrial NAD-dehydrogenases [38]. Furthermore, this enzyme was shown to exhibit the lowest sensitivity to inhibition by NADH [38]. Similar results were obtained with *A. thaliana* NAD-ME2, which displays high $K_m$ NAD and $K_i$ NADH values (Table 1) [17]. Thus, despite not competing effectively for the pool of NAD in the mitochondrial matrix under conditions of low levels of this substrate, the enzyme would be able to oxidize L-malate when NADH levels are high and inhibitory to other mitochondrial dehydrogenases.

### Kinetic mechanism of NAD-ME1: alternative pathways for the ternary complex

The activity of NAD-ME1 in the direction of malate decarboxylation, examined at several NAD concentrations and at a saturating fixed level of L-malate, showed a hyperbolic response (Figure 3A). Nevertheless, a sigmoidal behaviour was observed when varying the L-malate concentration at a saturating level of NAD (Figure 3B). Thus the kinetic behaviour of NAD-ME1 was different from that observed for NAD-ME2.

In order to infer a possible reaction mechanism of NAD-ME1, initial-velocity studies were performed by varying the concentrations of NAD or L-malate while keeping the other substrate concentration at a subsaturating level. The results obtained indicated that at a low L-malate concentration (3.0 mM) the kinetic behaviour of NAD-ME1 was sigmoidal (Figure 3C), whereas at a low NAD concentration (1 mM) a complex kinetic behaviour was obtained (Figure 3D). In this latter case, with increasing L-malate concentration, the reaction velocity initially increased, reached a maximum, and subsequently declined (Figure 3D). The data obtained fitted to eqn (1), which presents second-degree terms for the substrate concentration. This kinetic behaviour could be explained by assuming that NAD and L-malate

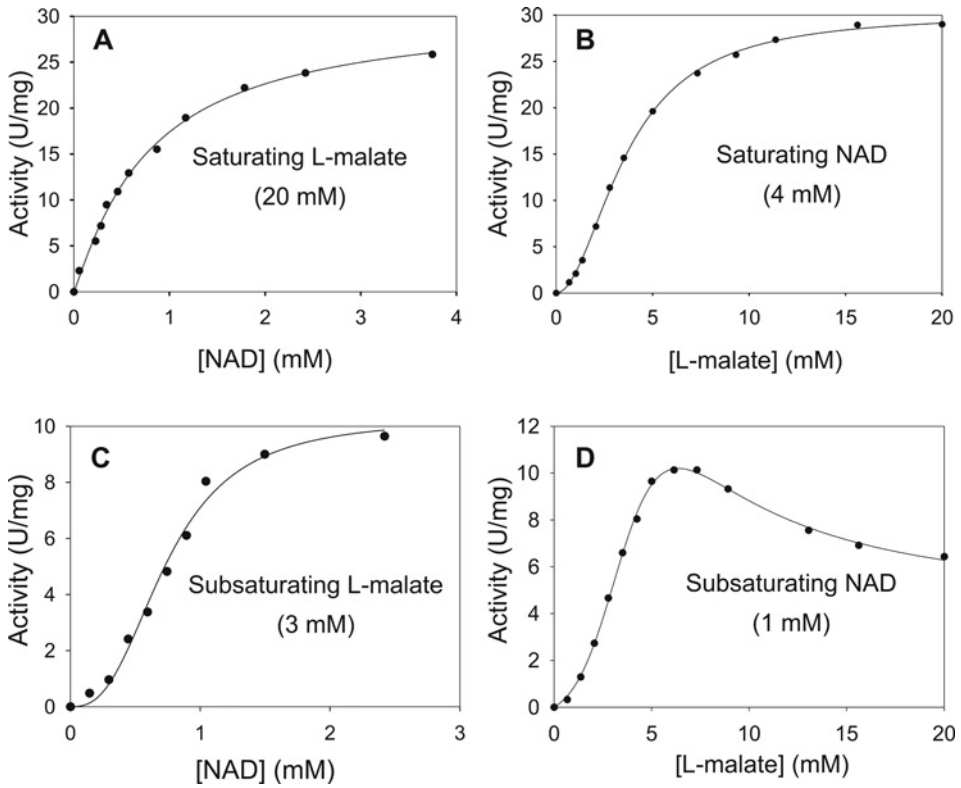


**Figure 3 Velocity plots against substrate concentration of *A. thaliana* NAD-ME1**

The enzymatic activity was determined at varying concentrations of L-malate or NAD and fixed levels of the other substrate (indicated in each case). Typical results from at least three independent determinations are shown.

combine with two different enzymatic species, suggesting a non-ordered sequential mechanism for NAD-ME1.

To analyse this hypothesis further, the forward enzymatic activity of NAD-ME1 was measured by varying simultaneously the free concentration of NAD (between 0.5 and 2.4 mM) and L-malate (between 1.0 and 7.3 mM) while keeping the metal concentration fixed (10 mM). When the resulting data matrix was fitted to eqn (4) (for a steady-state random Bi-Ter kinetic mechanism), the standard errors were lower than those obtained by using eqns (2) and (3). The results obtained suggest that each substrate combines to NAD-ME1 to give a binary complex, which then combines with the other substrate to give the ternary complex that breaks down to yield products (Figure 2B). However, the breakdown of this complex is not the sole rate-determining step, as there may be alternative pathways for the formation of the ternary complex (Figure 2B). In this regard, the data obtained indicate that the mechanism of NAD-ME1 may involve the binding of NAD before L-malate as the preferred pathway for the formation of the ternary complex (Figures 3 and 2B). In this kinetic model, at a subsaturating concentration of L-malate, the enzyme would be present in two forms: E (free enzyme) or E-MAL (enzyme linked to L-malate). In this condition, at low NAD concentrations the route followed is almost entirely the less favourable kinetic pathway, which first involves the formation of the E-MAL complex (Figure 2B). But, when the NAD concentration increases, the kinetically preferred route begins to take over, indicated by the upward lift in the rate curve (Figure 3C). As the NAD concentration is further increased, the enzyme becomes saturated with NAD and the reaction velocity curve reaches a plateau. This model is also represented by the sigmoidal relationship between velocity and NAD concentration (Figure 3C).

This proposed kinetic model for NAD-ME1 also explains how at a subsaturating NAD concentration, the velocity of the reaction initially increases with increasing L-malate concentrations, reaches a maximum and finally declines (Figure 3D). This means that the substrate flux initially passes through the more favourable pathway (with NAD binding first) to the less favourable one as the enzyme becomes saturated with L-malate, with reduction of the overall velocity (Figure 2B). A similar kinetic model has been observed for other enzymes, namely phosphofructokinase and glutathione reductase [39,40].

### The interaction between NAD-ME1 and -ME2 generate a heteromeric enzyme NAD-MEH with a particular kinetic behaviour

The analysis presented above indicated that NAD-ME1 and -ME2 show different kinetic mechanisms: the substrates bind randomly to NAD-ME1, but with a favoured kinetic route, whereas NAD-ME2 exhibits a sequential ordered mechanism (Figure 2). As NAD-ME1 and -ME2 subunits can associate *in vivo* and *in vitro* to generate the active heterodimeric enzyme, NAD-MEH, the kinetic mechanism of this enzymatic entity was also analysed.

Like NAD-ME1, NAD-MEH showed a hyperbolic response to varying NAD concentrations at a saturating L-malate level, whereas a sigmoidal behaviour was displayed when the L-malate concentration was varied at a saturating level of NAD (Figures 4A and 4B). However, when initial-velocity studies were performed Q4 by varying the NAD or L-malate concentration while keeping the other substrate at a subsaturating level, the results obtained were

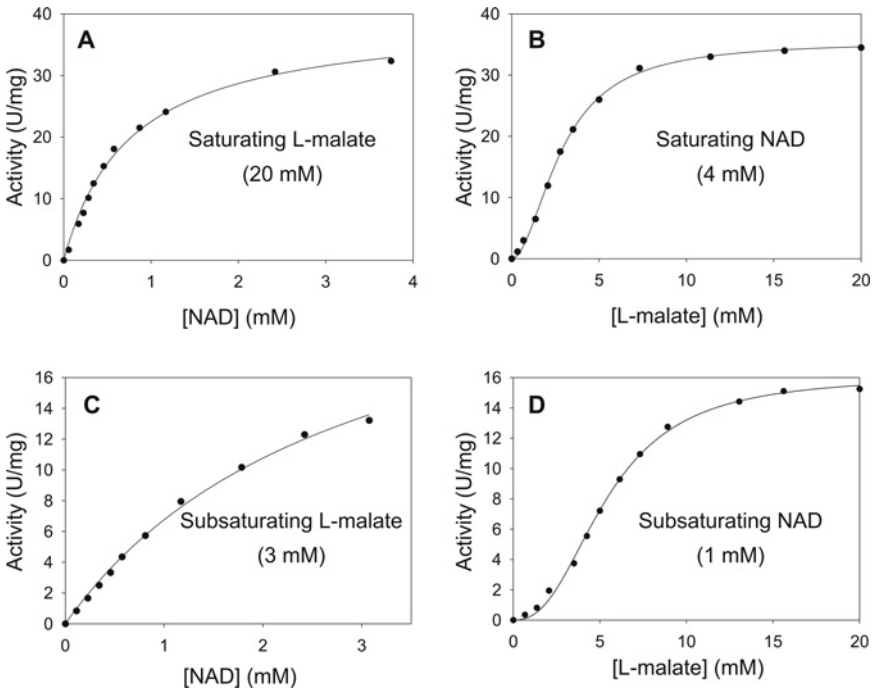


**Figure 4 Velocity plots against substrate concentration of *A. thaliana* NAD-MEH**

The enzymatic activity was determined at varying concentrations of L-malate or NAD and fixed levels of the other substrate (indicated in each case). Typical results from at least three independent determinations are shown.

similar to that observed at a saturating substrate level (Figure 4). In this regard, at low and high L-malate concentrations (3 and 20 mM respectively), the kinetic behaviour of NAD-MEH was hyperbolic (Figures 4A and 4C), while at low and high NAD concentrations (1 and 4 mM, respectively) a sigmoidal kinetic behaviour was observed (Figures 4B and 4D).

Finally, NAD-MEH results obtained when varying simultaneously the free concentration of NAD (between 0.5 and 2.4 mM) and L-malate (between 1 and 7.3 mM) were best fitted to eqn (4), as the standard errors were lower than those obtained with eqns (2) and (3). Thus, as in the case of NAD-ME1, NAD-MEH follows a non-sequential Bi-Ter kinetic mechanism where each substrate combines with the free enzyme to originate a binary complex to which the other substrate can bind (Figure 2C). However, the formation of the ternary complex would not follow a preferred route as in the case of NAD-ME1. NAD-MEH shows the same kinetic behaviour at low substrate levels (Figure 4), possibly because the ternary complex breakdown is the rate-determining step.

### The N-terminal region of NAD-ME1 and -ME2 is associated with the order of substrate binding

NAD-ME1 and -ME2 show the major primary structural divergence at the N-terminal region [18]. Moreover, the characterization of chimaeric proteins between both isoforms indicated that amino acid residues from this region are involved in substrate binding [18]. To gain information about the relationship between the amino acid sequence and the differences in the mechanism of reaction of both enzymes, a detailed kinetic study of NAD-ME1q [18], a chimaeric NAD-ME, was performed. NAD-ME1q is composed of the first 176 amino acid residues of NAD-ME2 and the central and C-terminal sequence of NAD-ME1 (Figure 5) [9].

Like NAD-ME2, NAD-ME1q showed a hyperbolic behaviour for L-malate and NAD (Figure 5A). When the forward enzymatic activity of NAD-ME1q was analysed by varying simultaneously the free concentration of NAD (between 0.3 and 3.2 mM) and L-malate (between 0.08 and 2.0 mM) the representation of data according to Lineweaver–Burk plots suggests that the reaction occurs through a sequential mechanism (Figure 4B). In agreement with this, the initial-velocity data best fitted to eqn (2), which describes a Bi-Ter ordered mechanism.

The type of product-inhibition pattern of NAD-ME1q obtained when NAD and L-malate were varied at several fixed concentrations of the three products (pyruvate, $CO_2$ or NADH) supports also the sequential ordered mechanism. In this regard, NADH (at 100 and 200 $\mu$M) showed competitive and mixed-type inhibition when NAD and malate were the variable substrates respectively (results not shown). Furthermore, pyruvate inhibition (at 10 and 50 mM) was uncompetitive with respect to NAD and mixed with respect to L-malate (results not shown). The pattern of $CO_2$ inhibition (at 2.8 and 11.2 mM) with respect to both, NAD or L-malate, was mixed (results not shown). This inhibition pattern Q5 obtained for NAD-ME1q was similar to that shown by the parental enzyme NAD-ME2.

Thus NAD-ME2 and NAD-ME1q follow a sequential ordered Bi-Ter mechanism, with NAD as the leading substrate (Figure 2A). These proteins share the N-terminal region (Figure 5A), indicating that this segment of the primary sequence is involved in the mode of substrate binding and is responsible for the differences observed between the kinetic mechanisms of each homodimer. It is possible that residues of the N-terminal end of NAD-ME2 are responsible for the inability of the free enzyme to bind L-malate. On the other hand, it cannot be ruled out that amino acid residues from the N-terminal end of NAD-ME1 are involved in L-malate binding in the absence of NAD.

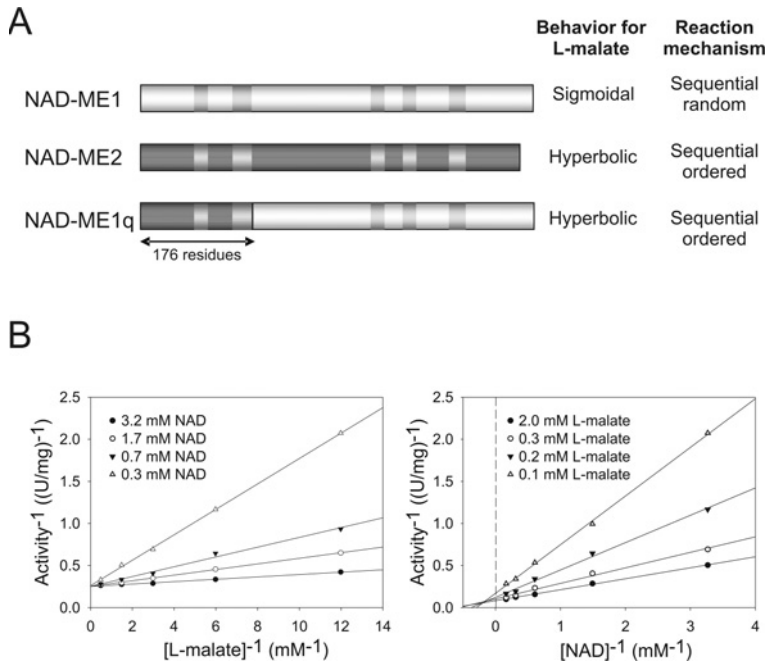


**Figure 5 Kinetic properties and mechanism of NAD-ME1q**

(**A**) NAD-ME1q was constructed with the first 176 amino acid residues from NAD-ME2 followed by the rest of the sequence corresponding to NAD-ME1 [18]. The kinetic behaviour with respect to malate and the reaction mechanism of NAD-ME1q and parental proteins are indicated on the right. The highly conserved sites found in NAD(P)-MEs are indicated as parallel gray bars. (**B**) Enzyme activity of NAD-ME1q was determined at varying concentrations of L-malate or NAD and fixed levels of the other substrate (see insets). Double-reciprocal plots are shown, as hyperbolic kinetics were obtained in all cases. Typical results from at least three independent determinations are shown.

### *A. thaliana* NAD-MEs do not decarboxylate OAA and have very low activity for the reductive carboxylation of pyruvate

The catalysis by NAD(P)-MEs generally proceeds in three steps: dehydrogenation of L-malate to OAA; decarboxylation of OAA to enolpyruvate; and finally tautomerization of enolpyruvate to pyruvate [1]. As a possible consequence of this mechanism, NAD(P)-MEs can also catalyse alternative reactions such as the OAA decarboxylation and the pyruvate reductive carboxylation [31,41]. In our previous work, the OAA decarboxylating activity could not be detected under standard conditions for recombinant NAD-ME1, -ME2 and -MEH [17,18]. In the present work, the OAA decarboxylation by NAD-ME1, -ME2 and -MEH was assayed in the presence of NAD or NADH (at 0.1 mM) in the reaction system. The rational behind this approach was that (i) it is known that NADP stimulates the OAA decarboxylation catalysed by pigeon liver NADP-ME [18], and (ii) assuming that NAD-ME1 and -ME2 follow the same three-step mechanism as NADP isoforms, NADH could be necessary for the second step (decarboxylation of OAA) during the catalysis. The results obtained indicated that the three *A. thaliana* NAD-MEs do not catalyse the decarboxylation of OAA, even in the presence of NAD or NADH.

The fact that all plant NAD-MEs characterized until now cannot decarboxylate OAA suggests that these enzymes possess a different kinetic mechanism to other NAD(P)-MEs, which can decarboxylate OAA as part of the chemical mechanism of catalysis (EC 1.1.1.40 and EC 1.1.1.38). In this regard, it is possible that OAA is not an intermediate of the reaction and that the dehydrogenation and decarboxylation would be concerted. On the other hand, it cannot be ruled out that EC 1.1.1.39-type NAD-MEs follow the same catalytic process described above, and the inability of these enzymes to catalyse OAA decarboxylation could be due to the inability to bind this compound from the medium. In any case, as plant NAD-MEs have been found only in mitochondria, their inability to use OAA may prevent decarboxylation of this organic acid, which is found at high concentrations within this organelle.

The capacity of the recombinant NAD-MEs to catalyse the pyruvate reductive carboxylation was analysed with different buffer systems. NAD-ME1, -ME2 and -MEH carboxylate pyruvate at a very low rate (0.05 U/mg, 0.02 U/mg and 0.05 U/mg respectively) in the presence of 50 mM pyruvate, 30 mM $NaHCO_3$, 0.2 mM NADH and 10 mM $MnCl_2$, pH 6.5. In none of the other conditions tested could the reverse activity be detected, even if the assays were repeated with different batches of the enzyme and at both low and high enzyme concentrations. The addition of 0.5 mM L-malate or 2 mM fumarate to the reaction medium had no effect on the reverse activity. These compounds act as activators of *A. suum* NAD-ME in the reverse sense of the reaction [42]. All together, these results indicate that these enzymes do not catalyse the pyruvate reductive carboxylation under physiological conditions.

In contrast to this, *A. thaliana* NADP-ME isoforms are able to catalyse the pyruvate reductive carboxylation at high rates and exhibit $K_m$ values for pyruvate of the same order of magnitude as the concentrations of this compound found in plants [23]. Recently, it was shown that the N-terminal end of *A. thaliana* NADP-ME2 is involved in the catalysis of the reductive carboxylation, as the deletion of the first 44 amino acids of the enzyme leads to a complete loss of the capacity to catalyse such a reaction [18]. This segment is not present in plant NAD-MEs, what could explain the very low reverse activity of the mitochondrial isoforms. The NAD-ME of *C. argentea* is the only enzyme from a plant source in which reverse activity was reported [35]. In this case, the carboxylase activity was less than 1.5 % of the forward

decarboxylase activity and the enzyme showed very low affinity toward the substrates pyruvate and $HCO_3^-$ [35]. In agreement with this, *A. thaliana* NAD-ME reverse activities were 0.05–0.16 % of the forward activity. In this way, plant mitochondrial NAD-MEs would play an exclusive catabolic role *in vivo*.

### Differential kinetic mechanisms of each NAD-ME in *A. thaliana*

Previous studies indicated that recombinant *A. thaliana* NAD-ME1 and -ME2 and -MEH behave differentially in terms of kinetic and regulatory properties [17,18]. The results presented in the present paper indicate that these enzymatic entities display different kinetic mechanisms, the binding of L-malate to NAD-ME1 and -MEH in the absence of NAD being one of the major differences compared with NAD-ME2. Moreover, other differences in the kinetic behaviour of NAD-ME1 and -MEH were observed (Figures 3 and 4), which imply a kinetically preferred pathway for the formation of the ternary complex in NAD-ME1 (Figure 2B). The binding of L-malate to NAD-ME1 and -MEH could be directly to the active site or, alternatively, to an allosteric site that is absent in NAD-ME2.

NAD-ME1 and -ME2 associate to generate a heterodimeric enzyme (NAD-MEH) with different regulatory properties from those shown by NAD-ME1 and -ME2 homodimers [18]. The results of the present work suggest that in NAD-MEH, each subunit may contribute to the interaction with the substrate in a different way. Essentially, the formation of the heterodimer appears to result in a change of the kinetic mechanism of NAD-ME2 to one similar to that shown by NAD-ME1. Another possibility could be that, despite the observation that the NAD-ME2 homodimer shows activity *in vivo* in the absence of NAD-ME1, the NAD-ME2 subunit may play a regulatory role rather than a catalytic one in the heterodimer, as was suggested previously for the $\beta$ subunit [16]. In either case, NAD-MEH is a new enzymatic entity whose properties are not described by those of the homodimers.

It is worth mentioning that the results obtained in this work are based on the use of recombinant enzymes. However, the kinetic parameters ($K_m$ and $k_{cat}$ values) and some regulatory properties displayed by these recombinant forms [17,18] are similar to those of characterized isofoms purified from several plant tissues [19]. Thus the *in vitro* approach suggests that, under metabolic conditions where the level of NAD is low and that of L-malate is high, the activity of NAD-ME2 and/or -MEH would be preferred over that of NAD-ME1. The different kinetic and regulatory properties shown by each *A. thaliana* NAD-ME further support the hypothesis of a specificity of function of each enzymatic entity in plant metabolism. In this way, although these proteins act in concert in most mature organs [17,18] they do not represent a case of functional redundancy.

## AUTHOR CONTRIBUTION

Marcos Tronconi, Mariel Gerrard Wheeler and María Drincovich designed the concept and experiments of this study. Marcos Tronconi prepared recombinant proteins and was specifically involved in data acquisition. Marcos Tronconi, Mariel Gerrard Wheeler, Verónica Maurino and María Drincovich were involved in the analysis and interpretation of the results. Carlos Andreo, in collaboration with the other authors, drafted the manuscript.

## FUNDING

This work was supported by Agencia Nacional de Promoción Científica y Tecnológica (ANPCyT), Argentina [grant number PICT 32233]; Consejo Nacional de Investigaciones Científicas y Técnicas (CONICET), Argentina; and the Deutsche Forschungsgemeinschaft, Germany.

## REFERENCES

1 Chang, G. G. and Tong, L. (2003) Structure and function of malic enzymes, a new class of oxidative decarboxylases. Biochemistry **42**, 12721–12733
2 Plaxton, W. C. and Podesta, F. E. (2006) The functional organization and control of plant respiration. Crit. Rev. Plant Sci. **25**, 159–198
3 Famiani, F., Walker, R. P., Tecsi, L., Chen, Z. H., Proietti, P. and Leegood, R. C. (2000) An immunohistochemical study of the compartmentation of metabolism during the development of grape (*Vitis vinifera* L.) berries. J. Exp. Bot. **51**, 675–683
4 Maurino, V. G., Saigo, M., Andreo, C. S. and Drincovich, M. F. (2001) Non-photosynthetic malic enzyme from maize: a constitutively expressed enzyme that responds to plant defense inducers. Plant Mol. Biol. **45**, 409–420
5 Lai, L. B., Wang, L. and Nelson, T. M. (2002) Distinct but conserved functions for two chloroplastic NADP-malic enzyme isoforms in C3 and C4 *Flaveria* species. Plant Physiol. **128**, 125–139
6 Shearer, H. L., Turpin, D. H. and Dennis, D. T. (2004) Characterization of NADP-dependent malic enzyme from developing castor oil seed endosperm. Arch. Biochem. Biophys. **429**, 134–144
7 Hurth, M. A., Suh, S. J., Kretzschmar, T., Geis, T., Bregante, M., Gambale, F., Martinoia, E. and Neuhaus, H. E. (2005) Impaired pH homeostasis in *Arabidopsis* lacking the vacuolar dicarboxylate transporter and analysis of carboxylic acid transport across the tonoplast. Plant Physiol. **137**, 901–910
8 Liu, S., Cheng, Y., Zhang, X., Guan, Q., Nishiuchi, S., Hase, K. and Takano, T. (2007) Expression of an NADP-malic enzyme gene in rice (*Oryza sativa* L.) is induced by environmental stresses; over-expression of the gene in *Arabidopsis* confers salt and osmotic stress tolerance. Plant Mol. Biol. **64**, 49–58
9 Chi, W., Yang, J., Wu, N. and Zhang, F. (2004) Four rice genes encoding NADP malic enzyme exhibit distinct expression profiles. Biosci. Biotechnol. Biochem. **68**, 1865–1874
10 Brown, N. J, Palmer, B. G., Stanley, S., Hajaji, H., Janacek, S. H., Astley, H. M., Parsley, K., Kajala, K., Quick, W. P., Trenkamp, S. et al. (2010) C4 acid decarboxylases required for C4 photosynthesis are active in the mid-vein of the C3 species *Arabidopsis thaliana*, and are important in sugar and amino acid metabolism. Plant J. **61**, 122–133
11 Xu, Y., Bhargava, G., Wu, H., Loeber, G. and Tong, L. (1999) Crystal structure of human mitochondrial NAD(P)$^+$-dependent malic enzyme: a new class of oxidative decarboxylases, Structure **7**, 877–889
12 Coleman, D. E., Jagannatha, Rao G. S., Goldsmith, E. J., Cook, P. F. and Harris, B. G. (2002) Crystal structure of the malic enzyme from *Ascaris suum* complexed with nicotinamide adenine dinucleotide at 2.3 Å resolution, Biochemistry **41**, 6928–6938
13 Grover, S. D. and Wedding, R. T. (1984) Modulation of the activity of NAD malic enzyme from *Solanum tuberosum* by changes in oligomeric state. Arch. Biochem. Biophys. **234**, 418–425
14 Willeford, K. O. and Wedding, R. T. (1987) Evidence of multiple subunit composition of plant NAD malic enzyme. J. Biol. Chem. **262**, 8423–8429
15 Burnell, J. N. (1987) Photosynthesis in phosphoenolpyruvate carboxykinase-type $C_4$ species: properties of NAD-malic enzyme from *Urochloa panicoides*. Aust. J. Plant Physiol. **14**, 517–525
16 Long, J. L., Wang, J. L. and Berry, J. O. (1994) Cloning and analysis of the $C_4$ photosynthetic NAD-dependent malic enzyme of *Amaranth* mitochondria. J. Biol. Chem. **269**, 2817–1833
17 Tronconi, M. A., Fahnenstich, H., Gerrard Wheeler, M. C., Andreo, C. S., Flügge, U. I., Drincovich, M. F. and Maurino, V. G. (2008) *Arabidopsis* NAD-malic enzyme functions as a homodimer and heterodimer and has a major impact during nocturnal metabolism. Plant Physiol. **146**, 1540–1552
18 Tronconi, M. A, Maurino, V. G, Andreo, C. S. and Drincovich, M. A. (2010) Three different and tissue- specific NAD malic enzymes generated by alternative subunit association in *Arabidopsis thaliana*. J. Biol. Chem. **285**, 11870–11879
19 Winning, B. M., Bourguignon, J. and Leaver, C. J. (1994) Plant mitochondrial NAD-dependent malic enzyme. J. Biol. Chem. **269**, 4780–4786
20 Douce, R. and Neuburger, M. (1989) The uniqueness of plant mitochondria. Annu. Rev. Plant Physiol. Plant Mol. Biol. **40**, 371–414
21 Palmer, J. M., Schwitzguébel, J. P. and Moller, I. M. (1982) Regulation of malate oxidation in plant mitochondria. Biochem. J. **208**, 703–711
22 Gerrard Wheeler, M. C., Arias, C. L., Tronconi, M. A., Maurino, V. G., Andreo, C. S. and Drincovich, M. F. (2008) *Arabidopsis thaliana* NADP-malic enzyme isoforms: high degree of identity but clearly distinct properties. Plant Mol. Biol. **67**, 231–242
23 Maurino, V. G., Gerrard Wheeler, M. C., Andreo, C. S. and Drincovich, M. F. (2009) Redundancy is sometimes seen only by the uncritical: does *Arabidopsis* need six malic enzyme isoforms? Plant Sci. **176**, 715–721

24 Gerrard Wheeler, M. C., Tronconi, M. A., Drincovich, M. F., Andreo, C. S., Flügge, U. I. and Maurino, V. G. (2005) A comprehensive analysis of the NADP-malic enzyme gene family of *Arabidopsis*. Plant Physiol, **139**, 39–51

25 Detarsio, E., Gerrard Wheeler, M. C., Campos Bermúdez, V. A., Andreo, C. S. and Drincovich, M. F. (2003) Maize $C_4$ NADP-malic enzyme. Expression in *Escherichia coli* and characterization of site-direct mutants at the putative nucleotide-binding sites. J. Biol. Chem. **278**, 13757–13764

26 Grover, S. D., Canellas, P. F. and Wedding, R. T. (1981) Purification of the NAD malic enzyme from potato and investigation of some physical and kinetic properties. Arch. Biochem. Biophys. **209**, 396–407

27 Dixon, M. and Webb, E. C. (1979) Enzymes (3rd edn), Academic Press, New York

28 Laemmli, U. K. (1970) Cleavage of structural proteins during the assembly of the head of bacteriophage T4. Nature **227**, 680–685

29 Fromm, H. J. (1979) Use of competitive inhibitors to study substrate binding order. Methods Enzymol. **63**, 467–486

30 Coombs, J., Baldry, C. W. and Bucke, C. (1973) The $C_4$ pathway in *Pennisetum purpureum*. Planta **110**, 109–120

31 Spampinato, C. P. and Andreo, C. S. (1995) Kinetic mechanism of NADP-malic enzyme from maize leaves. Photosynth. Res. **43**, 1–9

32 Hsu, R. Y. (1970) Mechanism of pigeon liver malic enzyme. J. Biol. Chem. **245**, 6675–6682

33 Chang, G. G., Huang, T. M., Wang, J. K., Lee, H. J., Chou, W. Y. and Meng, C. L. (1992) Kinetic mechanism of the cytosolic malic enzyme from human breast cancer cell line. Arch. Biochem. Biophys. **296**, 468–473

34 Teller, J. K., Fahien, L. A. and Davis, J. W. (1992) Kinetics and regulation of hepatoma mitochondrial NAD(P) malic enzyme. J. Biol. Chem. **267**, 10423–10432

35 Wedding, R. T. and Black, K. (1983) Physical and kinetic properties and regulation of the NAD malic enzyme purified from leaves of *Crassula argentea*. Plant Ph**y**siol. **72**, 1021–1028

36 Park, S. H., Kiick, D. M., Harris, B. G. and Cook, P. F. (1984) Kinetic mechanism in the direction of oxidative decarboxylation for NAD-malic enzyme from *Ascaris suum*. Biochemistry **23**, 5446–5453

37 Aktas, D. F. and Cook, P. F. (2008) Proper positioning of the nicotinamide ring is crucial for the *Ascaris suum* malic enzyme reaction. Biochemistry **47**, 2539–2546

38 Pascal, N., Dumas, R. and Douce, R. (1990) Comparison of the kinetic behavior toward pyridine nucleotides of NAD-linked dehydrogenases from plant mitochondria. Plant Physiol. **94**, 189–193

39 Ferdinand, W. (1966) The interpretation of non-hyperbolic rate curves for two-substrate enzymes. Biochem. J. **98**, 278–283

40 Bashir, A., Perham, R. N., Scrutton, N. S. and Berry, A. (1995) Altering kinetic mechanism and enzyme stability by mutagenesis of the dimmer interface glutathione reductase. Biochem. J. **312**, 527–533

41 Schimerlik, M. I. and Cleland, W. W. (1977) Inhibition and alternate-substrate studies on the mechanism of malic enzyme. Biochemistry **16**, 565–570

42 Karsten, W. E., Pais, J. E., Rao, G. S. J., Harris, B. G. and Cook, P. F. (2003) *Ascaris summ* NAD-malic enzyme is activated by malate and fumarate binding to separate allosteric sites. Biochemistry **42**, 9712–9721


Received 1 April 2010/1 June 2010; accepted 9 June 2010
Published as BJ Immediate Publication 9 June 2010, doi:10.1042/BJ20100497

Biochem. J. (2010) **430**, 00–00 (Printed in Great Britain) doi:10.1042/BJ20100497

online data

## SUPPLEMENTARY ONLINE DATA

# NAD-malic enzymes of *Arabidopsis thaliana* display distinct kinetic mechanisms that support differences in physiological control

Marcos A. TRONCONI*, Mariel C. GERRARD WHEELER*, Verónica G. MAURINO†, María F. DRINCOVICH* and Carlos S. ANDREO*[1]

*Centro de Estudios Fotosintéticos y Bioquímicos (CEFOBI), Universidad Nacional de Rosario, Suipacha 531, Rosario, Argentina, and †Botanisches Institut, Universität zu Köln, Zülpicher Str. 47b, 50674, Cologne, Germany.

[1] To whom correspondence should be addressed (carlosandreo@cefobi-conicet.gov.ar)

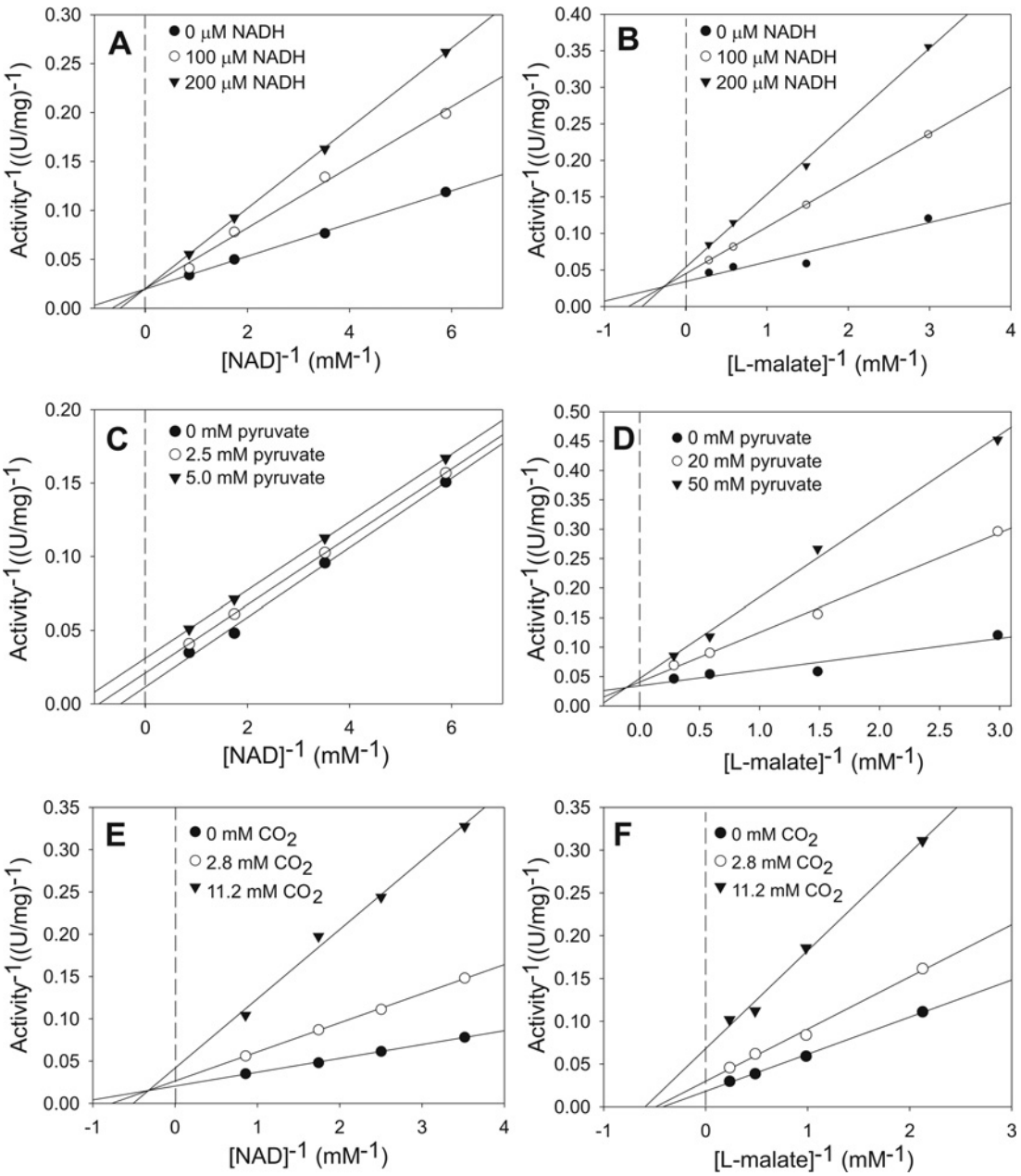


**Figure S1 Double-reciprocal plots for the inhibition by NADH, pyruvate or $NaHCO_3$ of NAD-ME2 activity**

The enzymatic activity of NAD-ME2 was determined using NAD as the variable substrate at 3.5 mM L-malate (**A**, **C** and **E**). The enzymatic activity of NAD-ME2 was determined using L-malate as the variable substrate at 0.6 mM NAD (**B**, **D** and **F**). In all cases, the concentrations of the inhibitors used are indicated. In the case of $NaHCO_3$, the calculated concentrations of $CO_2$ used are indicated. Typical results from at least three independent determinations are shown.

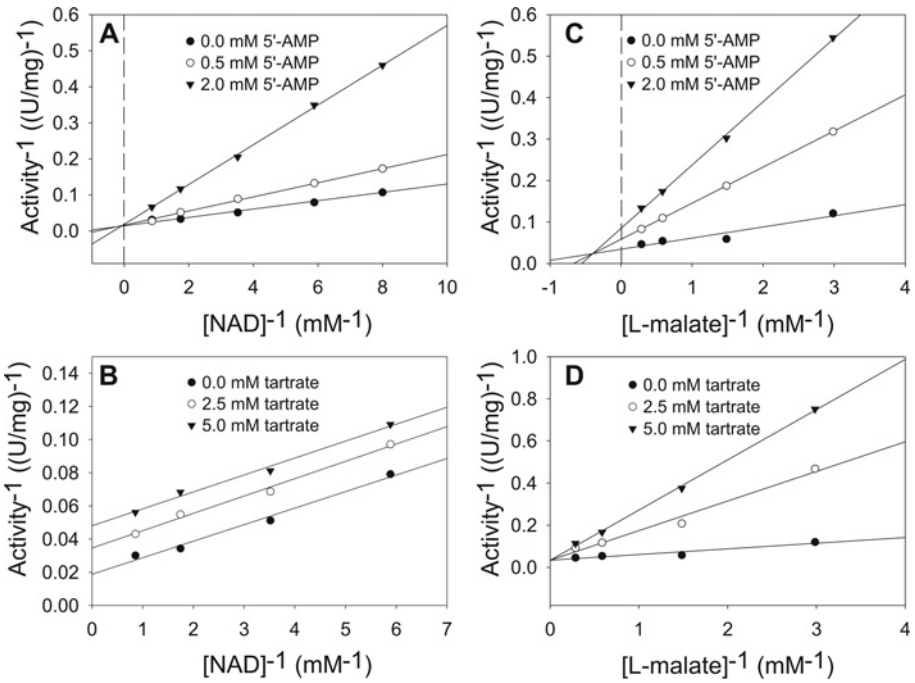


**Figure S2 Double-reciprocal plots for the inhibition by 5′-AMP and tartrate of NAD-ME2 activity**

The enzymatic activity of NAD-ME2 was determined using NAD as the variable substrate at 3.5 mM L-malate (**A** and **B**). The enzymatic activity of NAD-ME2 was determined using L-malate as the variable substrate at 0.6 mM NAD (**C** and **D**). In all cases, the concentrations of the inhibitors used are indicated. Typical results from at least three independent determinations are shown.

Received 1 April 2010/1 June 2010; accepted 9 June 2010
Published as BJ Immediate Publication 9 June 2010, doi:10.1042/BJ20100497